

Technical Report

Nr. HDA-da/sec-2013-001
March 21th, 2013



da/sec

BIOMETRICS AND INTERNET-SECURITY
RESEARCH GROUP



CASED

Template Ageing in Iris Biometrics:

**A Cross-Algorithm Investigation of the
ND-Iris-Template-Ageing-2008-2010 Database**

Authors

E. Ellavarason and C. Rathgeb

1 Introduction

There existed a belief in the iris biometric community about iris ageing - irises are immune to the vicissitudes of time. As time unfolded, various researches started proving that it is just an optimistic assumption; irises are affected by ageing factors. Thus, nullifying the notion of “single enrollment for life” concept, which is once the person’s iris is enrolled, the system can recognize them indefinitely. To put it in biometric terms, once enrolled, the chances of getting a false non-match error remains constant over time.

The formal definition of template ageing states “template ageing refers to the increase in error rates caused by time related changes in the biometric pattern, its presentation, and the sensor” [1]. Deteriorating imaging equipment, posture and environment influencing the dilation of the pupil are some of the factors responsible for iris template ageing. The discrepancies between the templates stored in biometric authentication systems and the data obtained from actual owners of the biometric templates affects the performance of the biometric system. Mostly the divergence is associated to within-person variations. There are many sources of iris ageing that have been identified such as cloudiness of the eye lens due to cataract, increase in blood pressure within the eyeball which is associated with glaucoma. Dealing with ageing in biometric systems represents a challenging task.

2 Research Goal

This paper deals with investigation of template ageing in iris biometrics. In order to carry out the research, experiments with a dataset of approximately three years of elapsed time between the most recent and the earliest iris image is taken into consideration. Based on the similarity scores generated by six different algorithms used in USIT (University of Salzburg Iris Toolkit)¹, match and non-match distributions are acquired for genuine and imposter image comparisons for short and long time span image comparisons. Statistical analysis is done for each category of dataset and results are presented. The results demonstrate the presence of template ageing in iris biometrics. Further, performance analysis of iris processing algorithms has been done.

Further work deals with determining if the ageing is subject-specific and also discussing possible countermeasures to deal with iris template ageing to minimize the deterioration in the long-term performance of biometric authentication systems.

3 Previous Work

The first experimental results of iris template ageing was published by Baker et al.[2]. The dataset for the experiments conducted by them contained 26 irises (13 subjects) with images acquired over the time period 2004-2008 using a LG 2200 iris sensor. The authors used IrisBEE matcher for evaluation and concluded that at the false accept rate of 0.01%, the false reject rate increased by 75% for long-time lapse.

¹USIT: University of Salzburg Iris Toolkit: <http://www.wavelab.at/sources/>

Tome-Gonzalez et al. followed experimenting on template ageing by acquiring iris images with one to four week time difference, using an LG 3000 sensor. They used Masek's iris matcher implementation, which revealed a weak overall performance. Their experiment was based on comparison of images of same and different sessions across four weekly sessions. They reported that at a false match rate(FMR) of 0.01%, there was an increase in false non-match rate(FNMR) of 8.5% to 11.3% for within-session matches and increase in FNMR of 22.4% to 25.8% for across session matches [3].

Fenker and Bowyer conducted experiments on 86 irises (43 subjects), imaged over a two-year period. Iris matchers - IrisBEE and VeriEye were used for analysis. IrisBEE matcher results showed an increase in false reject rate ranging from 157% at a Hamming distance threshold of 0.28 to 305% at 0.34. Whereas VeriEye matcher showed an increase in false reject rate from short to long time-lapse by 195% at a threshold of 0.3 fractional hamming distance and up to 457% at a Hamming distance threshold of 1 [4].

The result presented in this paper is an extension over previous work in several ways. The previous experiments done on iris template ageing are largely based on the tool called IrisBEE. This paper deals with experiments done on datasets using a different tool - USIT, which implements six exclusively chosen iris processing algorithms. The result also presents the diagnostic performance of short and long time lapse comparison tests using receiver operating characteristic curve for each algorithm in USIT.

4 Experiments

This section describes the undertaken experiments.

4.1 Image Dataset

The dataset used for the study of iris ageing is from ND-Iris-Template-Aging-2008-2010 ². The image dataset that was taken into consideration for this experiment is from the years 2008, 2009 and 2010. The iris images acquired are of equal subjects throughout three year time span. The subject age ranges from 22 to 56 years old. Sixteen subjects are male and seven are female. None of the subjects wore glasses during data acquisition; five wore contact lenses at all acquisition sessions [7].

The iris image set is divided into two categories, namely, short-time lapse (containing image pairs of two images taken within the same year, with no more than 3 months of time lapse between them) and long-time lapse (image pairs of two images taken within different years for example - 2008 and 2009). The iris image comparison is divided based on genuine (authentic) and imposter comparisons. Genuine comparisons are based on comparison of iris images of same subject at different time lapse, whereas imposter comparison is based on comparing iris image of different subjects.

The following figures : 1, 2, 3 are examples of iris images of the same subject (subject ID - 02463) taken in 2008, 2009, 2010.

²ND-Iris-Template-Aging-2008-2010: <http://www3.nd.edu/~cvrl/CVRL/>

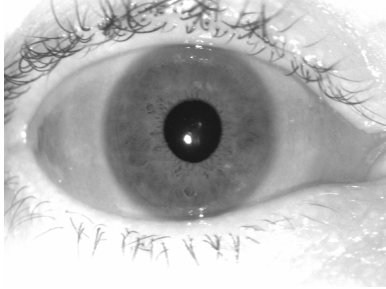


Figure 1: 2008.



Figure 2: 2009.

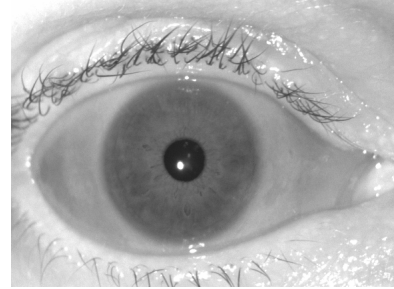


Figure 3: 2010.

Detailed information about the number of genuine and imposter iris images used for the experiments according to the time lapse is given in Table 1.

Time- Period (Year)	Number of Subjects	Number of Genuine Comparisons	Number of Imposter Comparisons
One year time lapse			
2008-2009 (short)	88	30346	30346
2008-2009 (long)	88	11931	11931
2009-2010 (short)	157	23901	23901
2009-2010 (long)	157	54472	54472
Two year time lapse			
2008-2010 (short)	40	5826	5826
2008-2010 (long)	40	14271	14271

Table 1: Table depicting the dataset used for the experiment.

4.2 Iris Matching Algorithms

In order to investigate the template ageing effects, USIT software package for iris recognition was used. This toolkit includes algorithms of iris preprocessing, feature extraction and comparison. The iris image undergoes iris detection, segmentation, preprocessing and feature extraction. The iris recognition tool applies pattern matching techniques to compare two iris images and retrieve a comparison score that reflects their degree of (dis-)similarity. The traditional iris processing chain adopted by this toolkit is depicted in Figure 4.

USIT uses different algorithms for iris segmentation, feature extraction and comparison. For this experiment, WAHET (Weighted Adaptive Hough and Ellipsopolar Transform) segmentation algorithm [14] is used.

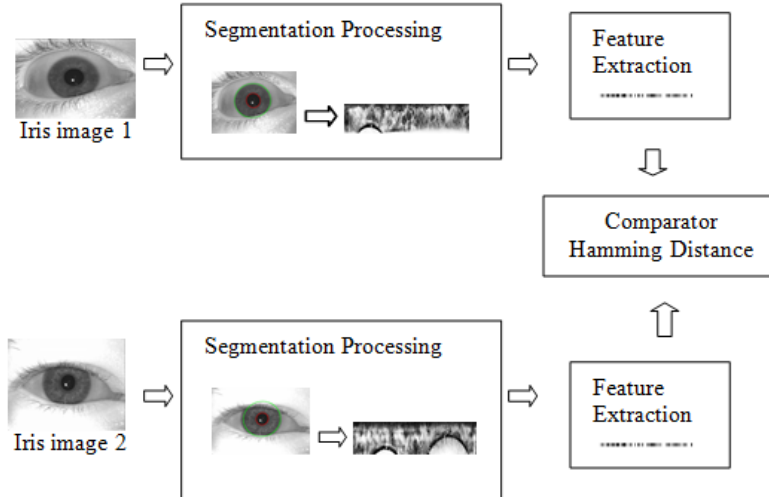


Figure 4: Iris Processing Chain.

For the feature extraction, the following six algorithms are used:

- Context-based Feature Extraction [8]
- Algorithm of Ko et al. [9]
- Algorithm of Ma et al. [10]
- 1D-LogGabor Feature Extraction [11]
- Algorithm of Monroe et al. [12]
- Algorithm of Rathgeb and Uhl [13]

4.3 Experimental Method

The experiment is divided into two phases: checking for evidence of template ageing and performance analysis of iris feature extraction algorithms.

4.3.1 Checking for evidence of template ageing

In order to get the iris textures, the iris images present in the dataset were subjected to segmentation process using WAHET segmentation algorithm. Then all six feature extraction algorithms were applied on the segmented textures for acquiring the iris code. Afterwards, the generated codes are compared based on the comparison algorithms such as Hamming distance based comparator and the similarity score is obtained. The range of the fractional Hamming distance score is between 0 to 1 with 0 being perfect match. Based on the similarity scores obtained, FMR and FNMR were calculated. Receiver operating characteristic graphs were drawn for one year time lapse and two year time lapse comparisons for each the algorithms. The curves obtained were compared for short and long time comparisons.

4.3.2 Performance analysis of iris feature extraction algorithms

Receiver operating characteristic graphs were drawn for each of the algorithms and the value of 1-FNMR at lower FMR rates such as 0.01%, 0.1% etc is calculated. Based on the result

obtained, the conclusion on which algorithm is the best is analysed.

Statistical Computation

For computing the verification rates namely FNMR, FMR and genuine match rate the following formulas were used [5]:

Φ_g is the set of all genuine similarity score

Φ_i is the set of all imposter similarity score

$\Phi_g(t)$ is the set of all genuine scores $s > t$

$\Phi_i(t)$ is the set of all imposter scores $s > t$

$$GMR(t) = \frac{\|\Phi_g(t)\|}{\|\Phi_g\|} \quad (1)$$

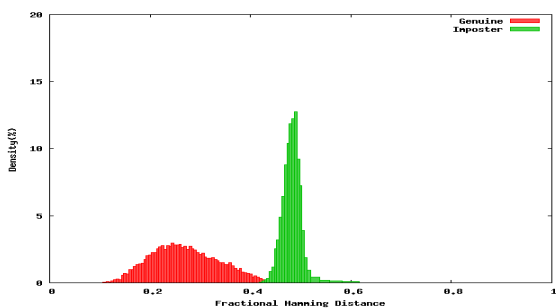
$$FMR(t) = \frac{\|\Phi_i(t)\|}{\|\Phi_i\|} \quad (2)$$

$$FNMR(t) = 1 - GMR(t) \quad (3)$$

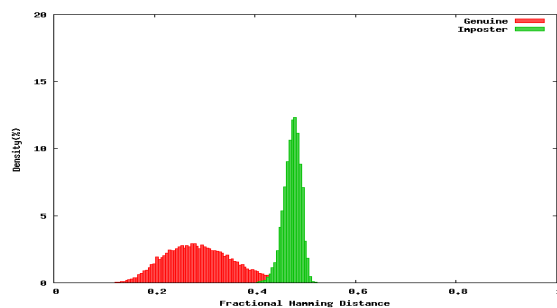
5 Results

5.1 Evidence of Template Ageing

In order to determine the presence of template ageing, various statistical experiments were carried out on the dataset. The first step was to determine the density distributions of the similarity scores for genuine and imposter comparison for each dataset for each algorithm in USIT. For each dataset, equal number of imposter and genuine image comparisons were considered. Imposter distribution were obtained by randomly comparing the iris image of two different subjects. The sample density histogram for 1D LogGabor algorithm for comparison of 2008-2009 short and long time lapses is shown in Figure 5.i and 5.ii.



i. Density distribution histogram of similarity scores for 1D LogGabor 2008-2009 short comparisons.



ii. Density distribution histogram of similarity scores for 1D LogGabor 2008-2009 long comparisons.

Figure 5: Graph Density Distribution Histogram of 1D LogGabor.

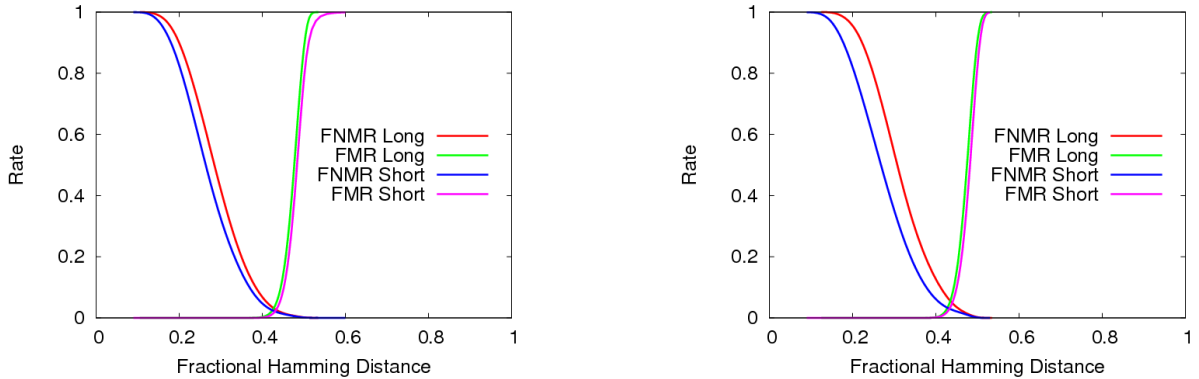
The density distribution for each of the short and long time comparisons for all the other algorithms were acquired in similar manner. These density distribution histogram graphs are provided in Appendix A.1.

Once the density distribution of the similarity scores were acquired, next step was to find out the FNMR and FMR. The graphs of the FNMR and FMR versus the similarity score are shown in Figure 6. The graphs are for FNMR and FMR change for one-year time lapse and two-year time lapse. The computation of FNMR and FMR is done by applying the the following formula on the genuine and imposter similarity score obtained for each dataset. Once the density distribution function was obtained for genuine scores, the FNMR and FMR are calculated using the following formulas:

$$FNMR(t) = \int_0^t \Phi_g(s) ds \quad (4)$$

$$FMR(t) = \int_t^1 \Phi_i(s) ds \quad (5)$$

where $\Phi_g(s)$ is the probability density distribution function of genuine similarity score S and $\Phi_i(s)$ is the probability density distribution function of imposter similarity score S for threshold t .



i. 1D LogGabor: FNMR and FMR versus Fractional Hamming Distance Short and Long comparisons 2008-2009.

ii. 1D LogGabor: FNMR and FMR versus Fractional Hamming Distance Short and Long comparisons 2008-2010.

Figure 6: Graph FNMR/FMR versus similarity score for 1D LogGabor.

The graphs shown in Figure 6 depict the comparison of the short time lapse (2008-2009-one year time lapse) and long time lapse (2008-2010-two year time lapse). As we can see from Figure 6, the gap between FNMR of short and long comparisons is increased for year 2008-2010. If there was no ageing factor involved, the FNMR curve for short and long comparison for year 2008-2010 should have stayed the same as year 2008-2009. But the fact that the resulting graph shows a gap between the FNMR rates for short and long term comparison shows the existence of ageing. The same experiment was conducted for all the

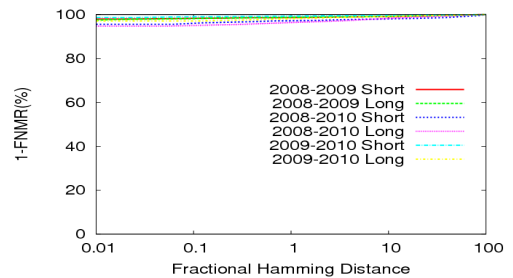
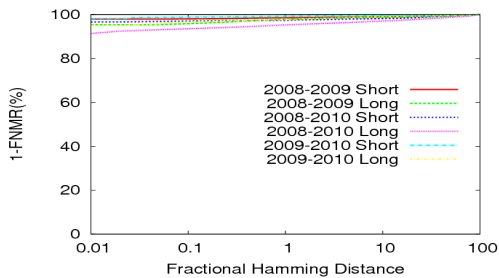
other algorithms and the result obtained clearly depicts the increasing gap of FNMR for short and long comparisons. The FNMR/FMR graphs for all other algorithms are provided in Appendix A.2. These graphs in Appendix A.2 depict the existence of iris template ageing factor using six different algorithms.

5.2 Performance Analysis of Algorithms

This part of the report deals with the performance analysis of different algorithms available in USIT. It is divided into two sections. First one is the analysis of individual algorithm and the second one gives the comparison of all of the algorithms with each other. While reporting the performance of any biometric system, it is important to consider the database, experimental protocol, etc. The performance can vary according to the nature and size of the database and hence the tests were conducted on three different datasets having comparisons within and across years.

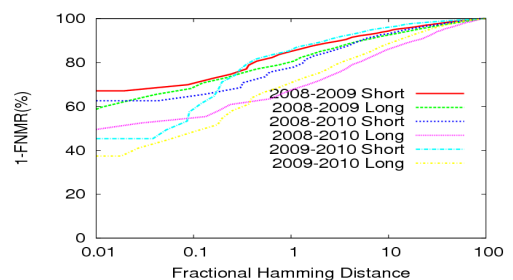
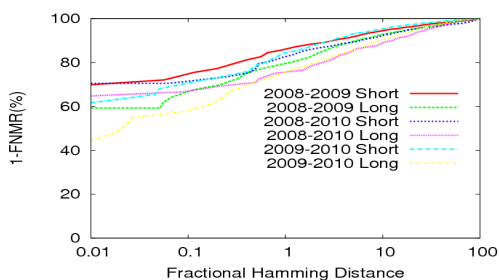
5.2.1 Individual Algorithm Performance Analysis

To evaluate the performance of iris image processing algorithms on the datasets, a receiver operating characteristic (ROC) curve is applied and further used for analyzing individual performance level for short and long term iris image comparisons.



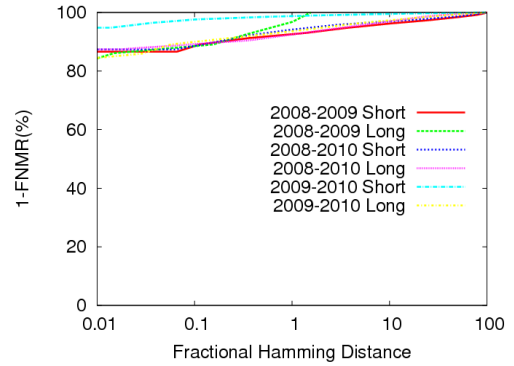
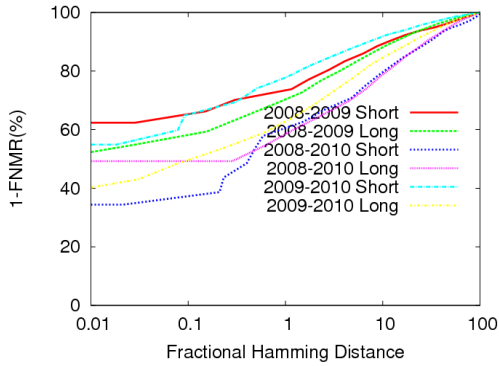
i. Receiver operating characteristic graph for short and long comparisons for 1D LogGabor algorithm.

ii. Receiver operating characteristic graph for short and long comparisons for algorithm Ma et al.



iii. Receiver operating characteristic graph for short and long comparisons for algorithm Ko et al.

iv. Receiver operating characteristic graph for short and long comparisons for Context-based algorithm.



v. Receiver operating characteristic graph for short and long comparisons for algorithm Rathgeb and Uhl.

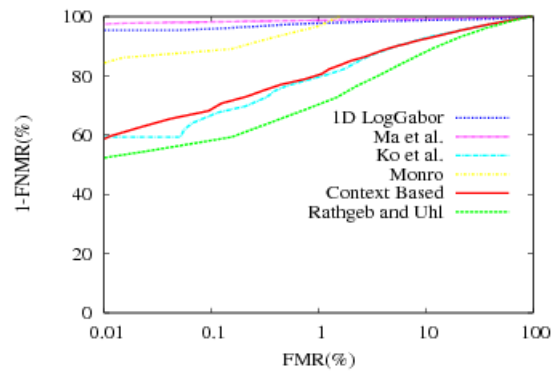
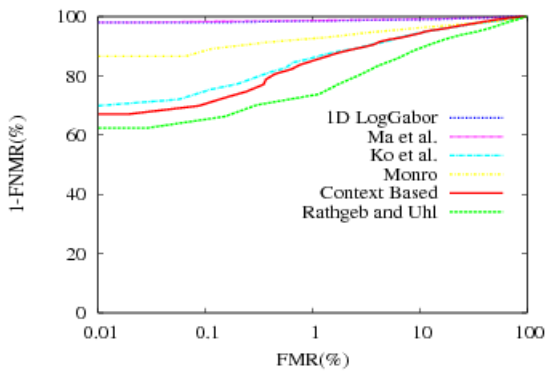
vi. Receiver operating characteristics graph for short and long comparisons for algorithm Monroe et al.

Figure 7: ROC for short and long time comparison for each algorithm.

As we can see from the above ROC graphs, the short time lapse comparison outperforms the long time lapse comparisons, the two year time lapse (2008-2010) comparisons have the lowest performance level compared to one-year time lapse comparisons (2008-2009 and 2009-2010).

5.2.2 Overall Performance Analysis

This section depicts values of 1-FNMR at lower FMR points for comparing different algorithms with each other. The graph is drawn for all six algorithm's short and long comparisons.



i. Receiver operating characteristic graph for the 2008-2009 short comparisons.

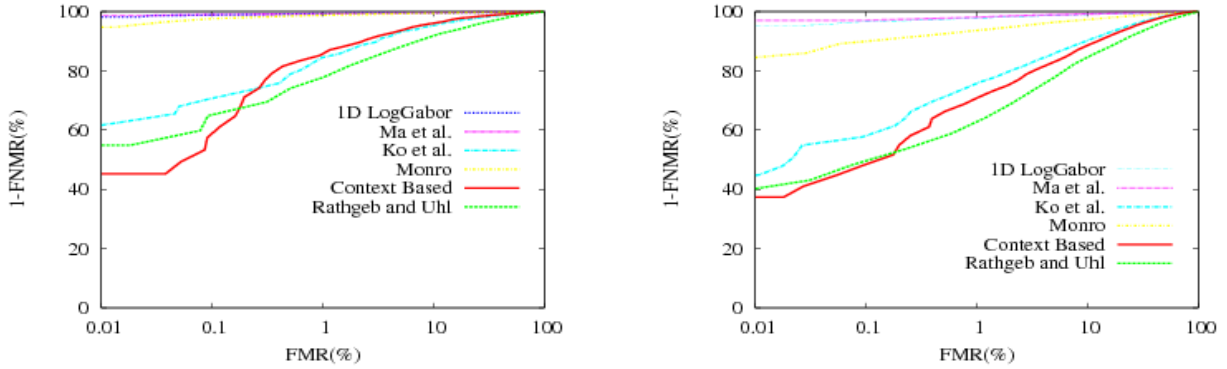
ii. Receiver operating characteristic graph for the 2008-2009 long comparisons.

Figure 8: Receiver operating characteristic graph for 2008-2009.

Table 2 gives the 1-FNMR values at low FMR's for 2008-2009.

Algorithm Type	FMR @ 0.01%	FMR @ 0.1%	FMR @ 1.0%
Short Comparison			
1-FNMR for 1D LogGabor	98.006449	98.153034	98.622104
1-FNMR for Monroe et al.	86.625574	89.051951	93.024165
1-FNMR for Ma et al.	98.006060	98.3970286	98.729351
1-FNMR for Rathgeb and Uhl	62.371688	66.252810	73.809756
1-FNMR for Ko et al.	69.803576	75.422652	87.168963
1-FNMR for Context-based	67.077103	72.686406	86.445812
Long Comparison			
1-FNMR for 1D LogGabor	94.51055	93.91215	97.199847
1-FNMR for Monroe et al.	86.084445	89.091795	96.790160
1-FNMR for Ma et al.	97.740388	98.534812	98.782132
1-FNMR for Rathgeb and Uhl	49.817963	59.056052	72.113172
1-FNMR for Ko et al.	55.204976	67.600989	80.416697
1-FNMR for Context-based	59.583083	70.695860	80.631373

Table 2: Verification results in terms of 1-FNMR at specific values of FMR for short time lapse comparison for year 2008-2009.



i. Receiver operating characteristic graph for the 2009-2010 short comparisons.

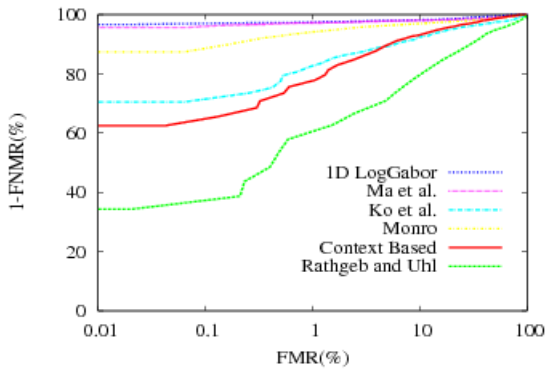
ii. Receiver operating characteristic graph for the 2009-2010 long comparisons.

Figure 9: Receiver operating characteristic graph for 2009-2010.

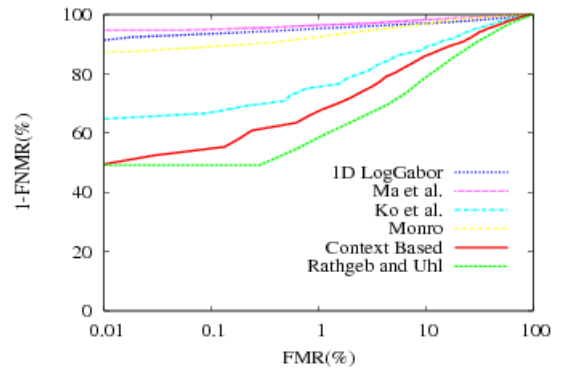
Table 3 gives the 1-FNMR values at the lower FMR's for 2009-2010.

Algorithm Type	FMR @ 0.01%	FMR @ 0.1%	FMR @ 1.0%
Short Comparison			
1-FNMR for 1D LogGabor	98.214367	98.863270	99.263656
1-FNMR for Monroe et al.	94.799576	97.611486	98.941506
1-FNMR for Ma et al.	98.674582	99.167011	99.341893
1-FNMR for Rathgeb and Uhl	54.908370	64.821806	77.893912
1-FNMR for Ko et al.	61.401810	73.730958	85.839201
1-FNMR for Context-based	45.280500	61.277555	85.213309
Long Comparison			
1-FNMR for 1D LogGabor	95.111228	96.997812	97.848322
1-FNMR for Monroe et al.	85.958866	91.826275	94.287229
1-FNMR for Ma et al.	96.332869	97.053040	98.228289
1-FNMR for Rathgeb and Uhl	38.166876	53.544524	64.031192
1-FNMR for Ko et al.	44.973159	61.495128	76.143769
1-FNMR for Context-based	37.381130	51.671016	71.009546

Table 3: Verification results in terms of 1-FNMR at specific values of FAR for short time lapse comparison for year 2009-2010.



i. Receiver operating characteristic graph for the 2008-2010 short comparisons.



ii. Receiver operating characteristic graph for the 2008-2010 long comparisons.

Figure 10: Receiver operating characteristics graph for 2008-2010.

Table 4 gives the 1-FNMR values at the lower FMR's for 2008-2010.

Algorithm Type	FMR @ 0.01%	FMR @ 0.1%	FMR @ 1.0%
Short Comparison			
1-FNMR for 1D LogGabor	96.652631	97.263157	97.347368
1-FNMR for Monro et al.	87.368421	89.978947	94.021052
1-FNMR for Ma et al.	95.578947	96.252631	97.136842
1-FNMR for Rathgeb and Uhl	34.361140	38.669482	62.745512
1-FNMR for Ko et al.	70.484210	73.494736	82.225000
1-FNMR for Context-based	62.568421	65.515789	77.873684
Long Comparison			
1-FNMR for 1D LogGabor	92.374508	94.358599	95.181494
1-FNMR for Monro et al.	87.452019	90.577590	94.004752
1-FNMR for Ma et al.	94.745019	96.380917	96.594955
1-FNMR for Rathgeb and Uhl	44.096143	49.241454	59.422406
1-FNMR for Ko et al.	64.668250	66.687991	75.059404
1-FNMR for Context-based	49.351124	55.355510	67.985743

Table 4: Verification results in terms of 1-FNMR at specific values of FAR for short time lapse comparison for year 2008-2010.

The accurate 1-FNMR% values at 0.01% FMR are given in tables 2, 3 and 4. Higher the 1-FNMR% value at 0.01% FMR, better the performance level. We can see from ROC graphs that algorithm Ma et al. and 1D LogGabor has the highest 1-FNMR% value. The curves for 1D LogGabor and Ma et al. algorithms almost coincide for all the three short time lapse graphs. But looking at the long time lapse graphs, it is clear that algorithm Ma et al.'s performance is better than all the other.

It is also important to notice that the performance of the Context-based feature extraction algorithm varies in 2008-2009, 2009-2010 and 2008-2010 graphs, as it outperforms performance of algorithm Rathgeb and Uhl in 2008-2009 and 2008-2010 but it does not in year 2009-2010 in both short and long comparisons. Overall, algorithms Ma et al., 1D LogGabor, Monro and Ko et al. have shown similar behavior in all the short and long comparisons, which enables us to draw a conclusion that algorithm Ma et al. performs better than all the other algorithms. Algorithm Rathgeb and Uhl shows a lowest performance level.

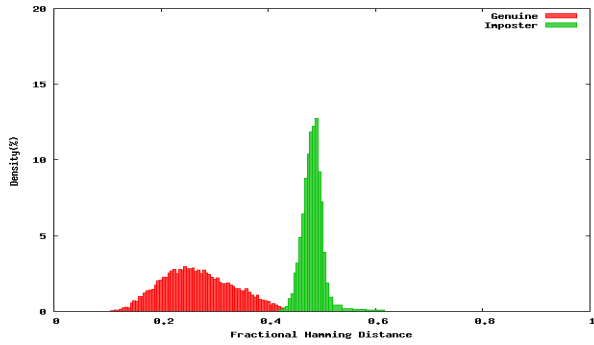
References

- [1] A.J. Mansfield and J.L. Wayman, *Best Practices in Testing and Reporting Performance of Biometric Devices*, NPL Report CMSC, 2002.
- [2] S. Baker, K.W. Bowyer and P.J. Flynn, *Empirical Evidence for Correct Iris match Score Degradation With Increased Time-Lapse Between Gallery and Probe Matches*, in *Proceedings of the International Conference on Biometrics*, pp. 1170-1179, 2009.
- [3] P. Tome-Gonzalez, F. Alonso-Fernandez and J. OrtegaGarcia, *The Effects of Time Variability in Iris Recognition*, *IEEE International Conference on Biometrics Theory, Applications and Systems*, 2008.
- [4] S.P. Fenker and K.W. Bowyer, *Experimental Evidence of Template Aging Effect in Iris Biometrics*, *IEEE Computer Society Workshop on Applications of Computer Vision*, 2011.
- [5] *Slides from Biometric Performance of Biometric Systems (DTU 02238)*, 2012.
- [6] C. Rathgeb, A. Uhl, and P. Wild, *Iris Recognition: From Segmentation to Template Security*, In *Advances in Information Security 59*. Springer, 2012.
- [7] S.P. Fenker and K.W. Bowyer, *Analysis of Template Aging in Iris Biometrics*, *IEEE Computer Society Biometrics Workshop*, 2012.
- [8] C. Rathgeb and A. Uhl, *Context-based Texture Analysis for Secure Revocable Iris-Biometric Key Generation*, *Proceedings of the 3rd International Conference on Imaging for Crime Detection and Prevention (ICDP'09)*, 2009.
- [9] J. Ko, Y. Gil, J. Yoo, and K. Chung, *A Novel and Efficient Feature Extraction Method for Iris Recognition*, *ETRI Journal*, Volume 29, No. 3, 2007.
- [10] Li Ma, T. Tan, Y. Wang and D. Zhang, *Efficient Iris Recognition by Characterizing Key Local Variations*, *IEEE Transaction on Image Processing*, Volume 13, No. 6, 2004.
- [11] L. Masek, *Recognition of Human Iris Patterns for Biometric Identification*, 2003.
- [12] D.M. Monro, S. Rakshit *DCT-Based Iris Recognition*, *IEEE Transaction on pattern analysis and machine intelligence*, Volume 29, No. 4, 2007.
- [13] C. Rathgeb and A. Uhl, *Secure Iris Recognition Based on Local Intensity Variations*, In *Proceedings of the International Conference on Image Analysis and Recognition (ICIAR'10)*, pp. 266-275, Springer LNCS, 6112, 2010.
- [14] A. Uhl and P. Wild, *Weighted Adaptive Hough and Ellipsopolar Transforms for Real-time Iris Segmentation*, In *proceedings of the 5th International Conference on Biometrics (ICB'12)*, pages 283-290, 2012 .

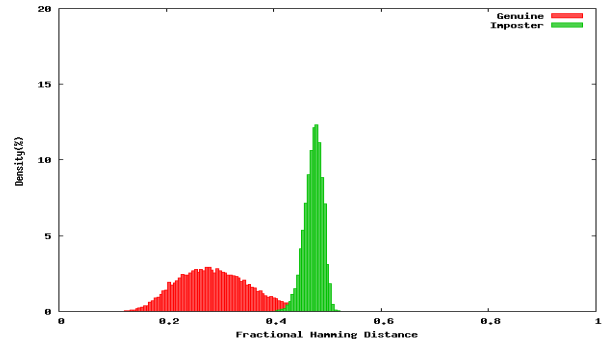
A Appendices

A.1 Appendix A

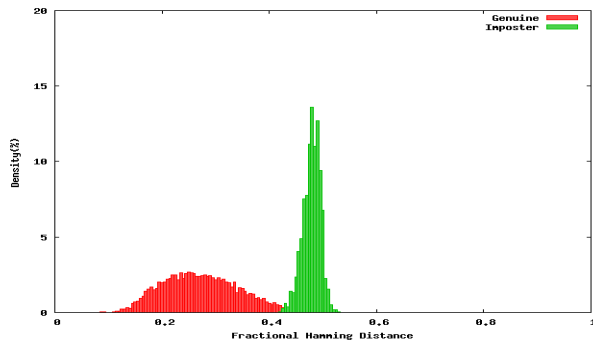
Figure 11: Graph of Density Distribution Histograms of 1D-LogGabor.



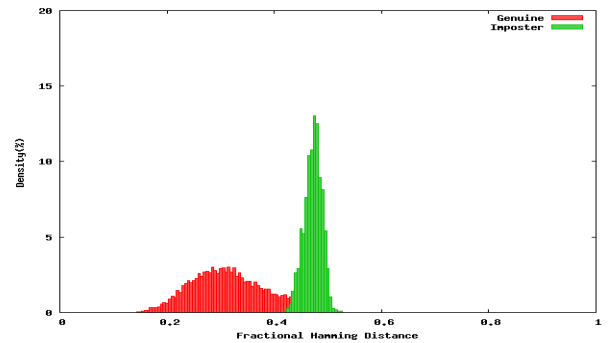
i. Density distribution histogram of similarity scores for 1D LogGabor 2008-2009 short comparisons.



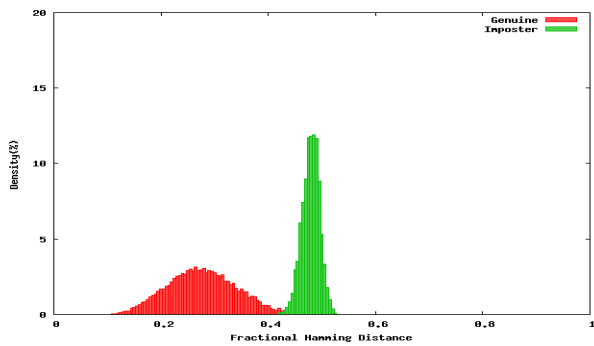
ii. Density distribution histogram of similarity scores for 1D LogGabor 2008-2009 long comparisons.



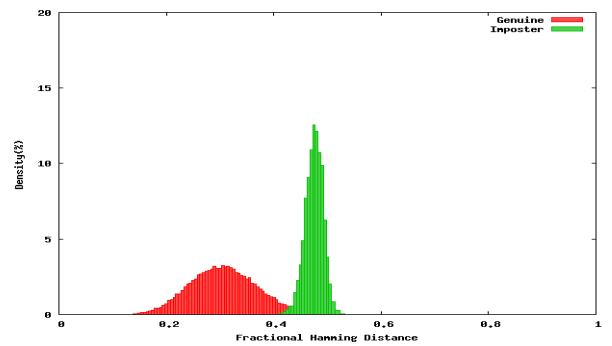
iii. Density distribution histogram of similarity scores for 1D LogGabor 2008-2010 short comparisons.



iv. Density distribution histogram of similarity scores for 1D LogGabor 2008-2010 long comparisons.

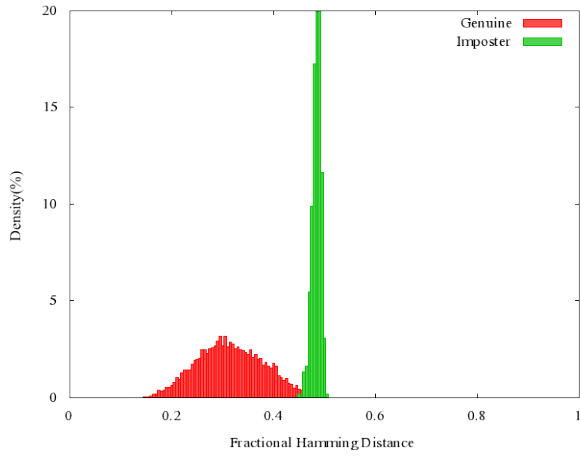


v. Density distribution histogram of similarity scores for 1D LogGabor 2009-2010 short comparisons.

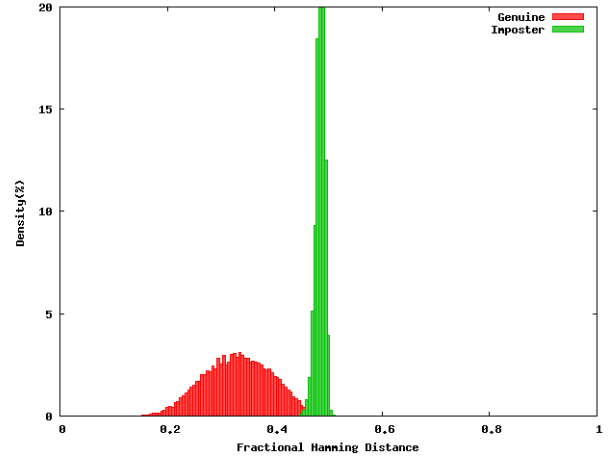


vi. Density distribution histogram of similarity scores for 1D LogGabor 2009-2010 long comparisons.

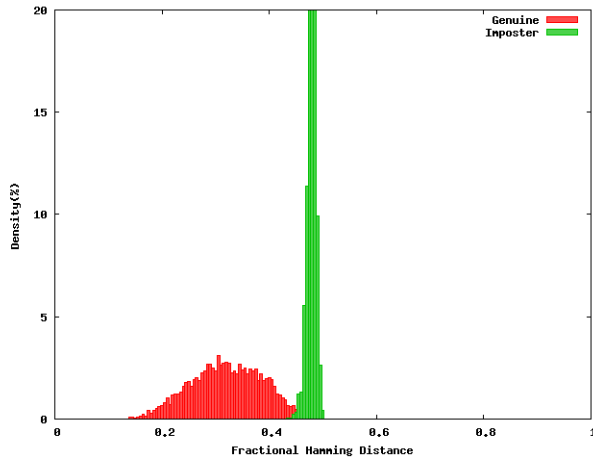
Figure 12: Graph of Density Distribution Histograms of Algorithm Ma et al.



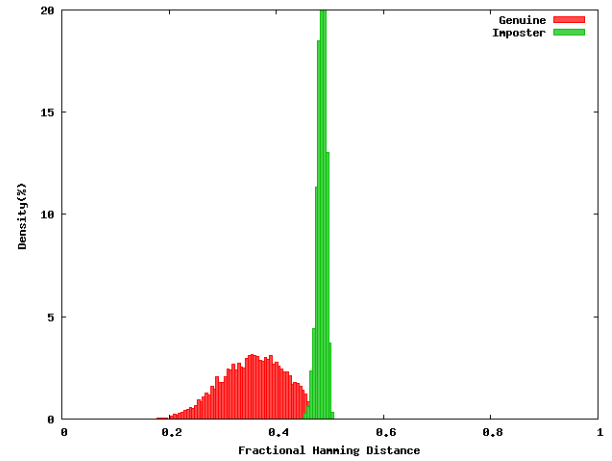
i. Density distribution histogram of similarity scores for Ma et al. 2008-2009 short comparisons.



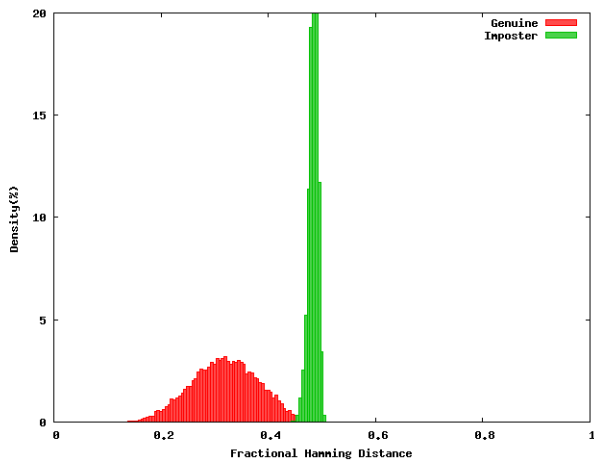
ii. Density distribution histogram of similarity scores for Ma et al. 2008-2009 long comparisons.



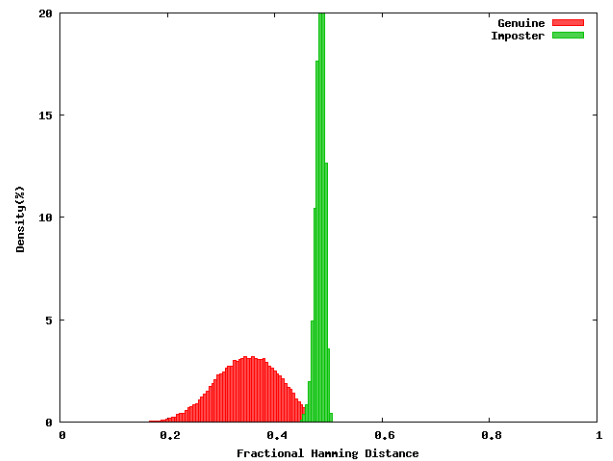
iii. Density distribution histogram of similarity scores for Ma et al. 2008-2010 short comparisons.



iv. Density distribution histogram of similarity scores for Ma et al. 2008-2010 long comparisons.

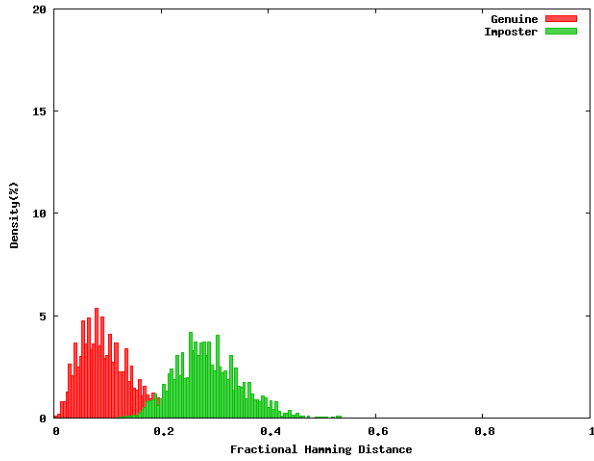


v. Density distribution histogram of similarity scores for Ma et al. 2009-2010 short comparisons.

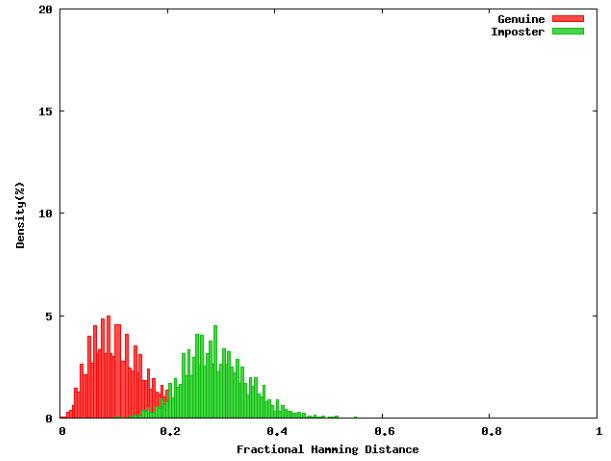


vi. Density distribution histogram of similarity scores for Ma et al. 2009-2010 long comparisons.

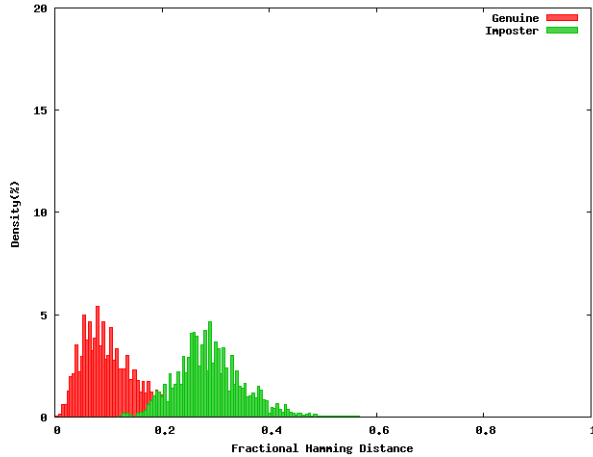
Figure 13: Graph of Density Distribution Histograms of Algorithm Ko et al.



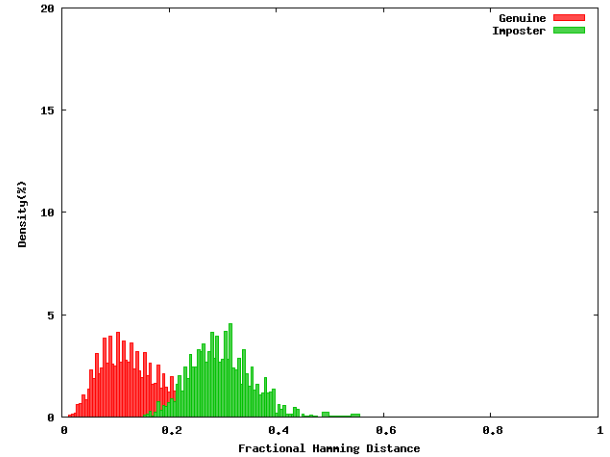
i. Density distribution histogram of similarity scores for Ko et al. 2008-2009 short comparisons.



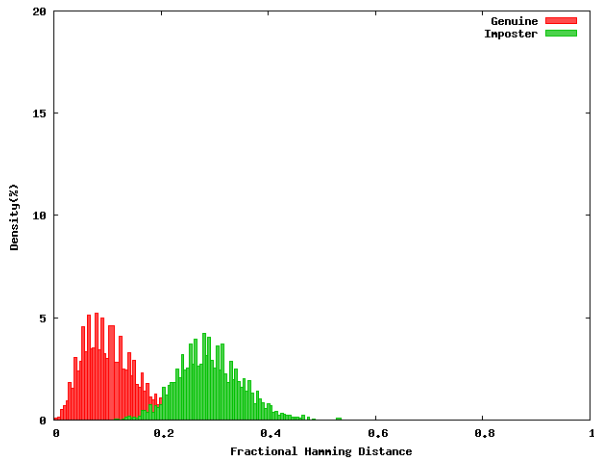
ii. Density distribution histogram of similarity scores for Ko et al. 2008-2009 long comparisons.



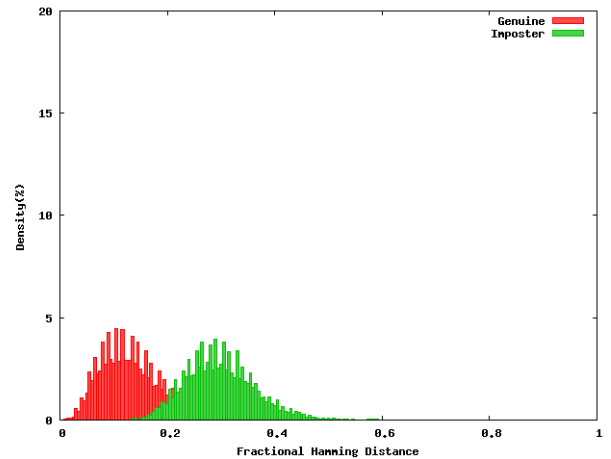
iii. Density distribution histogram of similarity scores for Ko et al. 2008-2010 short comparisons.



iv. Density distribution histogram of similarity scores for Ko et al. 2008-2010 long comparisons.

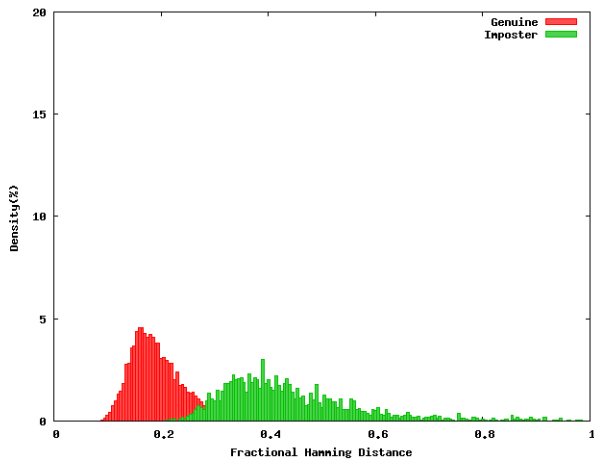


v. Density distribution histogram of similarity scores for Ko et al. 2009-2010 short comparisons.

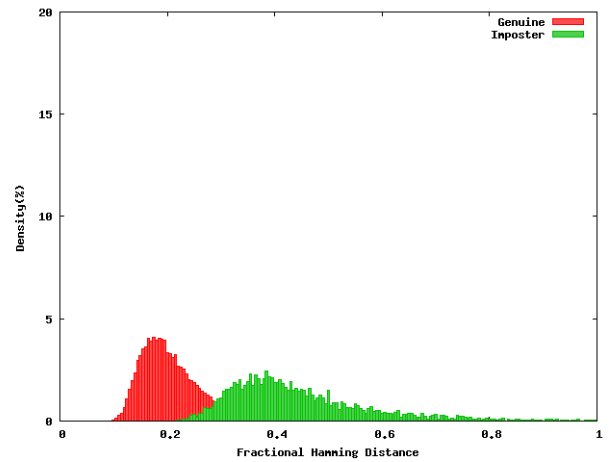


vi. Density distribution histogram of similarity scores for Ko et al. 2009-2010 long comparisons.

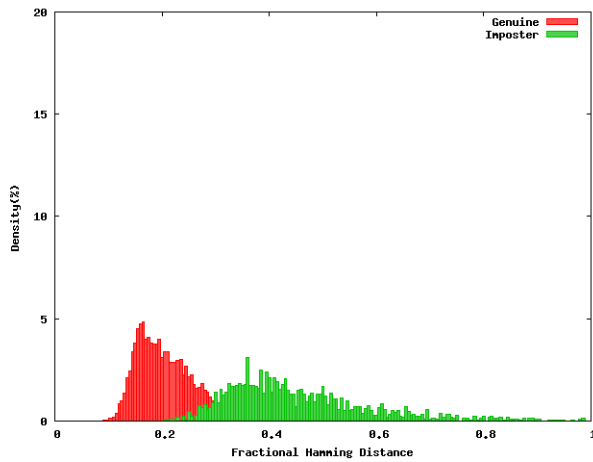
Figure 14: Graph of Density Distribution Histograms of Context-based algorithm



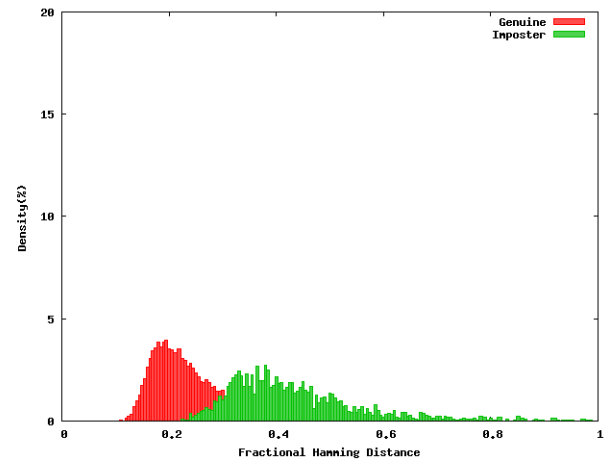
i. Density distribution histogram of similarity scores for Context-based algorithm 2008-2009 short comparisons.



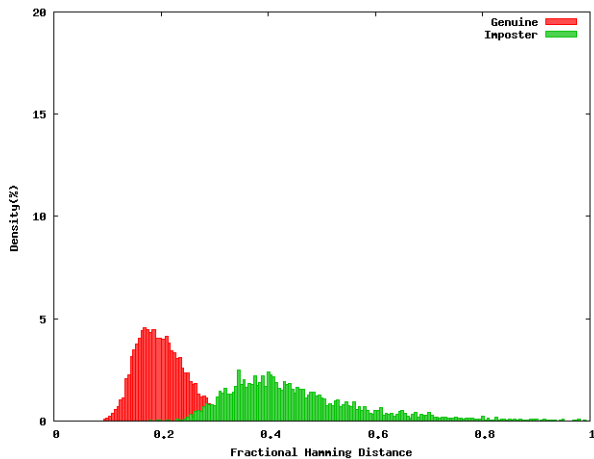
ii. Density distribution histogram of similarity scores for Context-based algorithm 2008-2009 long comparisons.



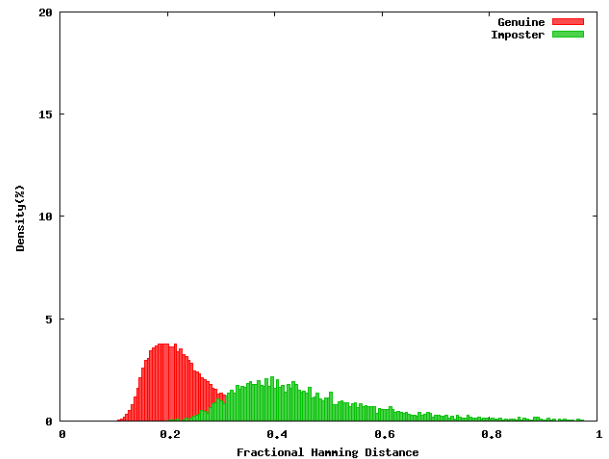
iii. Density distribution histogram of similarity scores for Context-based algorithm 2008-2010 short comparisons.



iv. Density distribution histogram of similarity scores for Context-based algorithm 2008-2010 long comparisons.

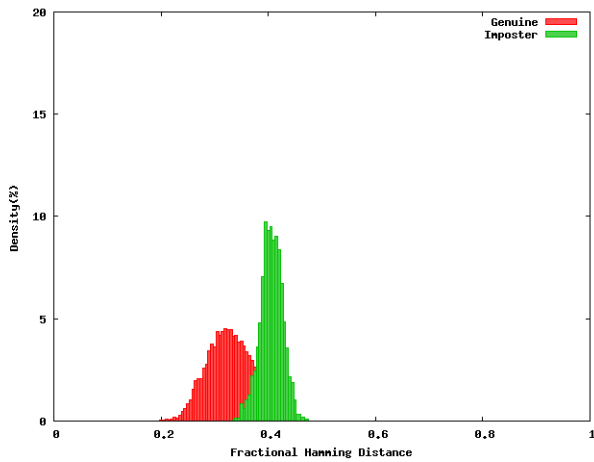


v. Density distribution histogram of similarity scores for Context-based algorithm 2009-2010 short comparisons.

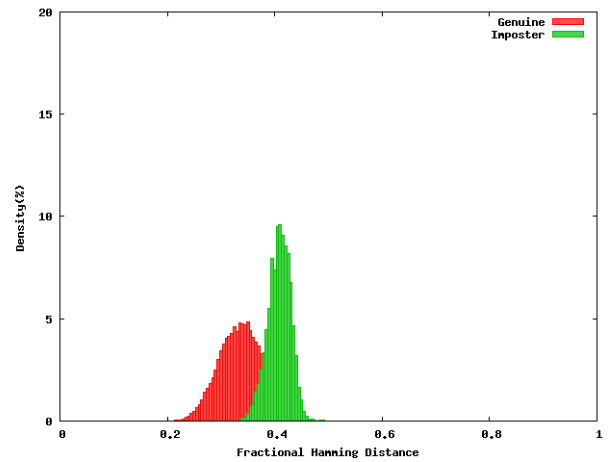


vi. Density distribution histogram of similarity scores for Context-based algorithm 2009-2010 long comparisons.

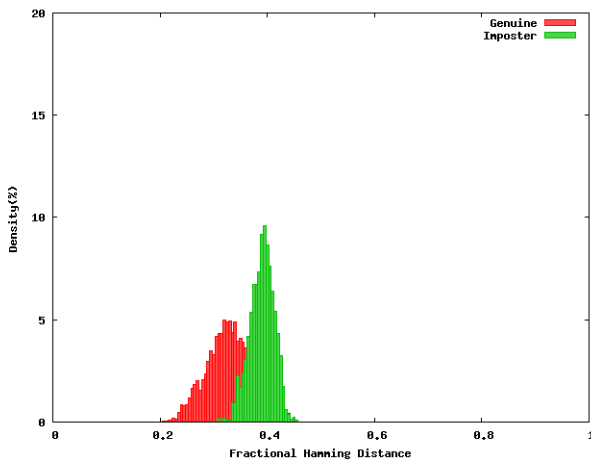
Figure 15: Graph of Density Distribution Histograms of Algorithm Rathgeb and Uhl



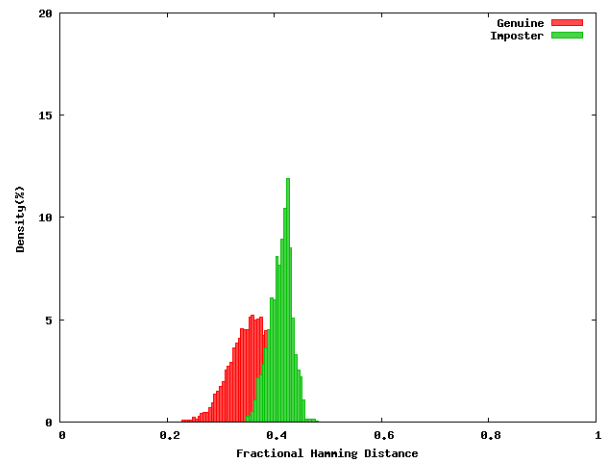
i. Density distribution histogram of similarity scores for algorithm Rathgeb and Uhl 2008-2009 short comparisons.



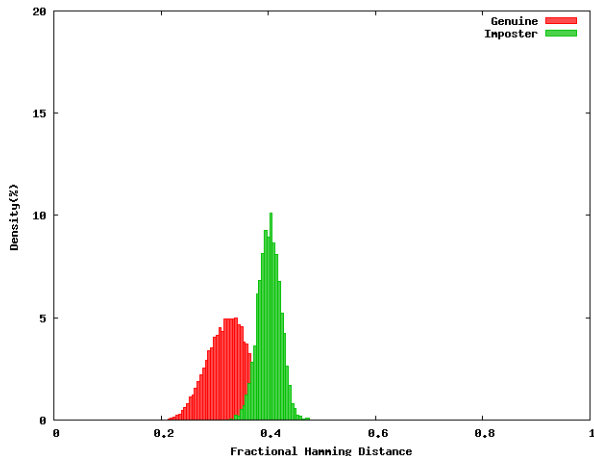
ii. Density distribution histogram of similarity scores for algorithm Rathgeb and Uhl 2008-2009 long comparisons.



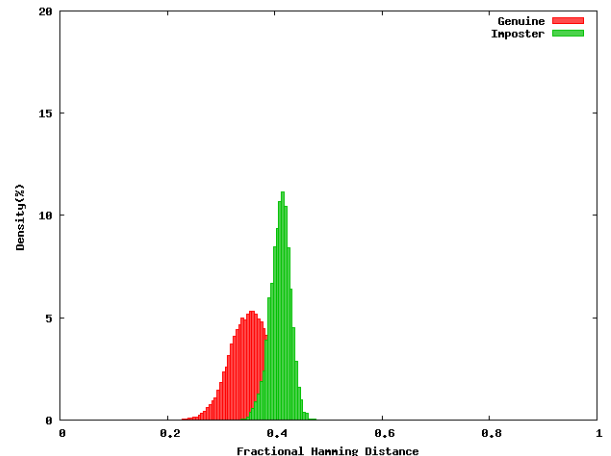
iii. Density distribution histogram of similarity scores for algorithm Rathgeb and Uhl 2008-2010 short comparisons.



iv. Density distribution histogram of similarity scores for algorithm Rathgeb and Uhl 2008-2010 long comparisons.

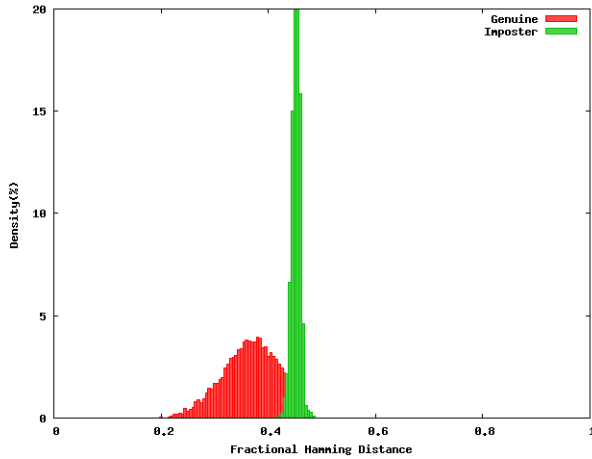


v. Density distribution histogram of similarity scores for algorithm Rathgeb and Uhl 2009-2010 short comparisons.

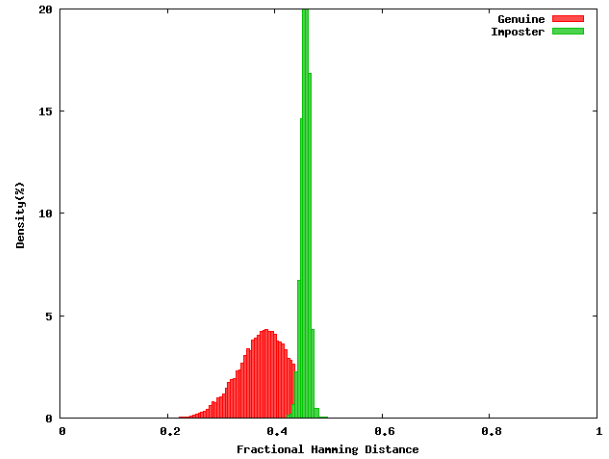


vi. Density distribution histogram of similarity scores for algorithm Rathgeb and Uhl 2009-2010 long comparisons.

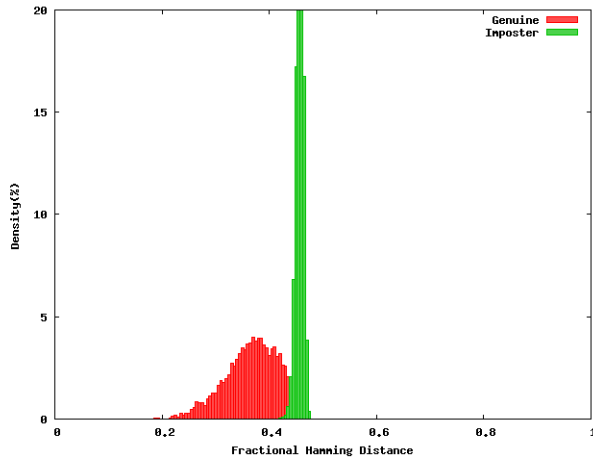
Figure 16: Graph of Density Distribution Histograms of Algorithm Monro et al.



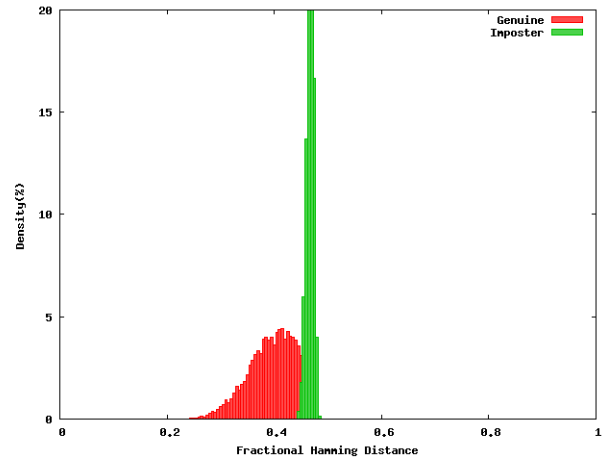
i. Density distribution histogram of similarity scores for algorithm Monro et al. 2008-2009 short comparisons.



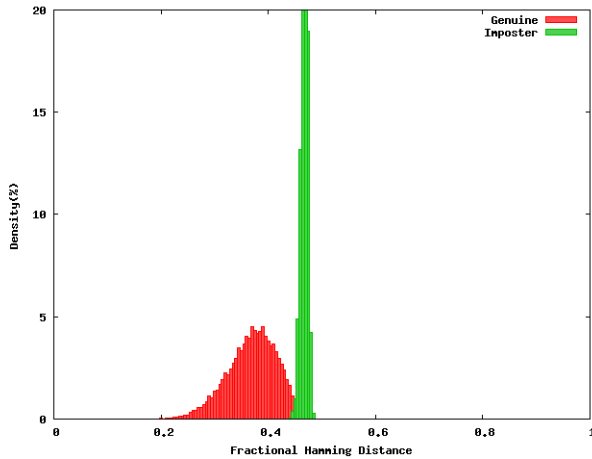
ii. Density distribution histogram of similarity scores for algorithm Monro et al. 2008-2009 long comparisons.



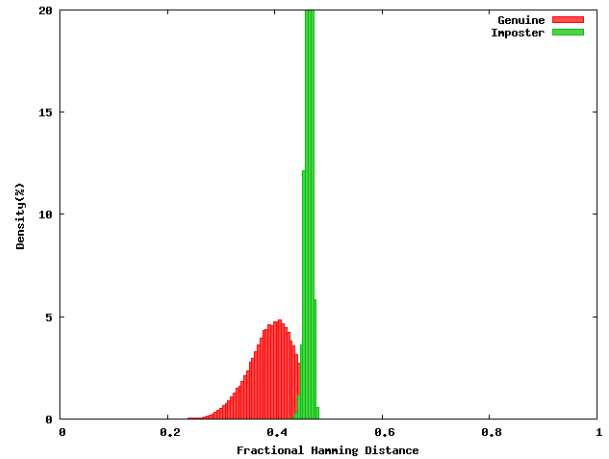
iii. Density distribution histogram of similarity scores for algorithm Monro et al. 2008-2010 short comparisons.



iv. Density distribution histogram of similarity scores for algorithm Monro et al. 2008-2010 long comparisons.



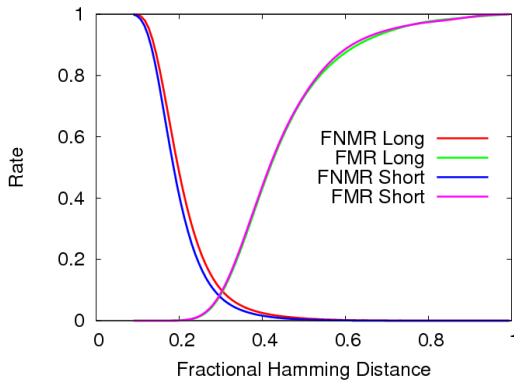
v. Density distribution histogram of similarity scores for algorithm Monro et al. 2009-2010 short comparisons.



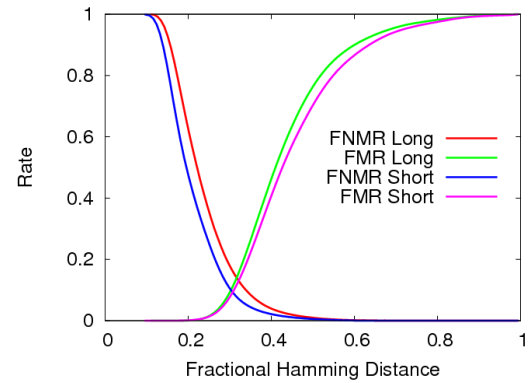
vi. Density distribution histogram of similarity scores for algorithm Monro et al. 2009-2010 long comparisons.

A.2 Appendix B

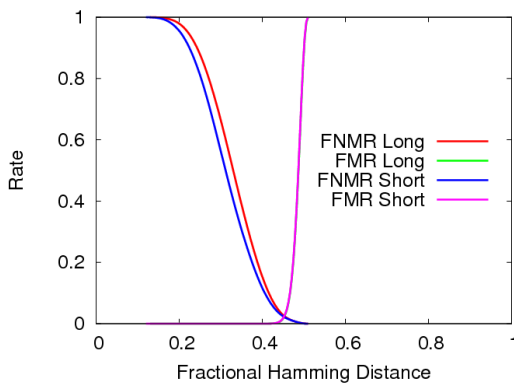
Figure 17: Graph FNMR/FMR versus Fractional Hamming Distance



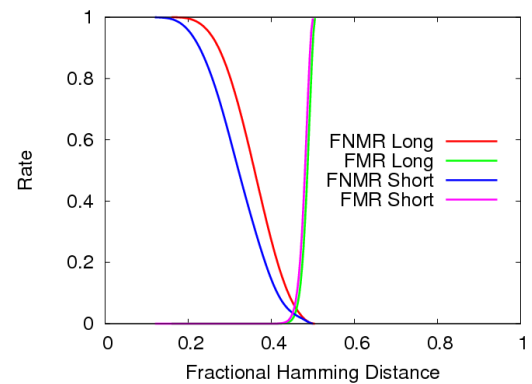
i. Context-based algorithm: FNMR and FMR versus Fractional Hamming Distance Short and Long comparisons 2008-2009.



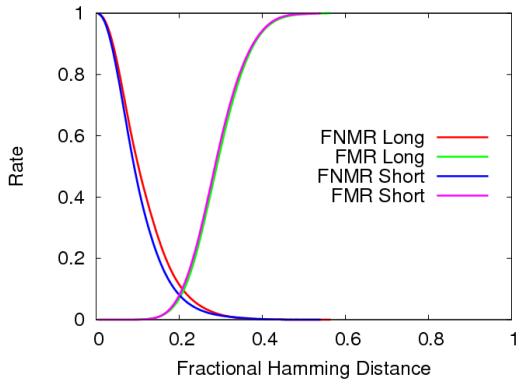
ii. Context-based algorithm: FNMR and FMR versus Fractional Hamming Distance Short and Long comparisons 2008-2010.



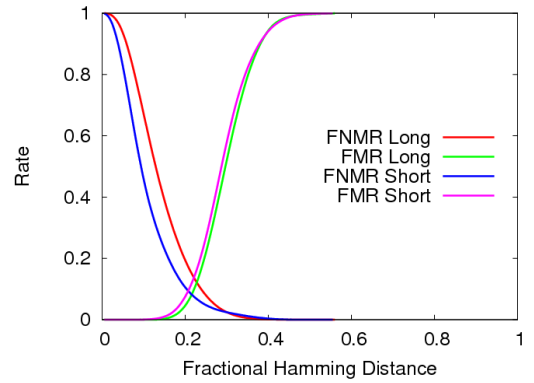
iii. Ma et al.: FNMR and FMR versus Fractional Hamming Distance Short and Long comparisons 2008-2009.



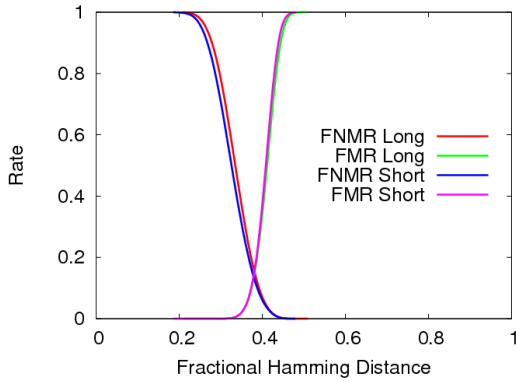
iv. Ma et al.: FNMR and FMR versus Fractional Hamming Distance Short and Long comparisons 2008-2010.



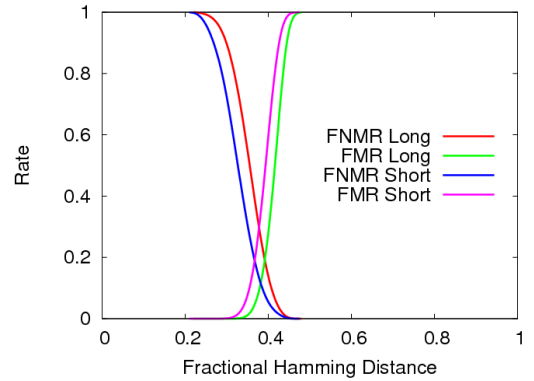
v. Ko et al.: FNMR and FMR versus Fractional Hamming Distance Short and Long comparisons 2008-2009.



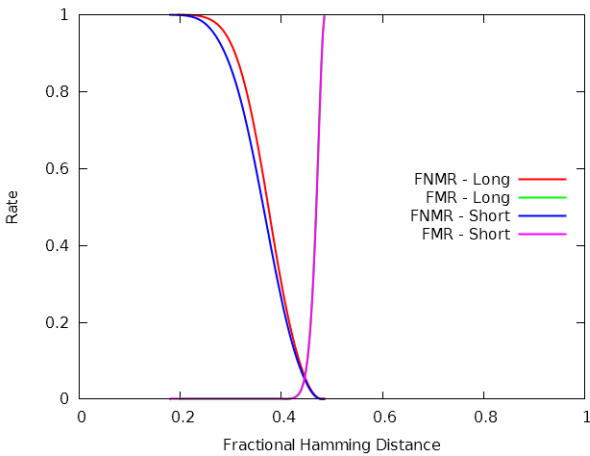
vi. Ko et al.: FNMR and FMR versus Fractional Hamming Distance Short and Long comparisons 2008-2010.



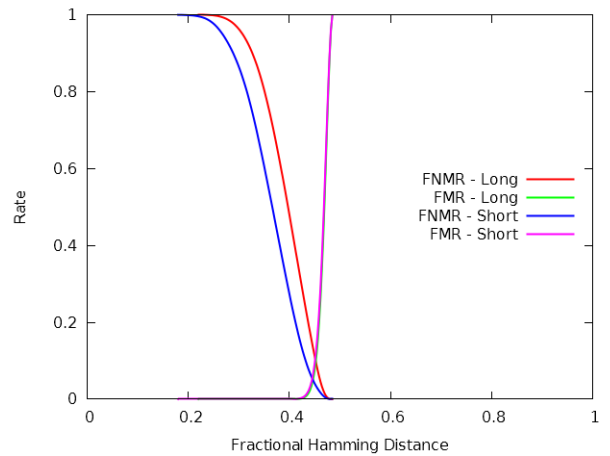
vii. Algorithm Rathgeb and Uhl: FNMR and FMR versus Fractional Hamming Distance Short and Long comparisons 2008-2009.



viii. Algorithm Rathgeb and Uhl: FNMR and FMR versus Fractional Hamming Distance Short and Long comparisons 2008-2010.



ix. Algorithm Monroe et al.: FNMR and FMR versus Fractional Hamming Distance Short and Long comparisons 2008-2009.



x. Algorithm Monroe et al.: FNMR and FMR versus Fractional Hamming Distance Short and Long comparisons 2008-2010.